How does Proteinase 3 bind to lipid bilayers? An *in silico* and *in vitro* study

Anne-Sophie Schillinger[1,2], Cédric Grauffel[1,2], Øyvind Halskau[1], Nathalie Reuter[1,2]

[1]Department of Molecular Biology, University of Bergen
[2]Computational Biology Unit, University of Bergen

Abstract

Proteinase 3 (PR3) is a serine proteinase from the human neutrophils that is expressed at the surface of the cell upon activation. The membrane expression of PR3 is associated with chronic inflammation diseases such as rheumatoid arthritis and vasculitis, but also in autoimmune diseases such as Wegener granulomatosis, where it is the main antigen of the anti-neutrophil cytoplasmic antibody (ANCAs). The modulation of PR3 membrane expression is highly relevant to the understanding of the role of PR3 in these pathologies and goes through the precise understanding of the binding mechanism between PR3 and the cell membrane, both at a macromolecular level but also at the atomic level. Here we show evidence of direct binding of PR3 towards POPC liposomes by Surface Plasmon Resonance (SPR) spectroscopy and precisely describe the molecular interactions that contribute to the direct binding of PR3 to POPC lipid bilayer with Molecular Dynamic (MD) simulations. Evidences are strongly supporting the hypothesis of direct binding of PR3 to lipid bilayers.

Introduction: Proteinase 3 is expressed at the membrane of the human neutrophils

Proteinase 3 (PR3) is a serine protease from the neutrophils that is found at the surface of the plasma membrane (Baggiolini, Bretz, Dewald, & Feigenson, 1978). It is know that this expression at the membrane is a risk factor for vasculitis and rheumatoid arthritis (Witko-sarsat et al., 1999). PR3, as a serine protease, has peptide bound cleavage activities and it was demonstrated that membrane bound PR3 is catalytically active against Boc-Alanine-Alanine-Norvaline-thiobenzyl ester and fibronectin, a component from the extracellular matrix (Campbell, Campbell, & Owen, 2000). Moreover, PR3 has been identified as a diagnosis marker in Wegener granulomatosis because it is recognized by anti-neutrophil cytoplasmic antibody (ANCAs) (Woude et al., 1985) and is now acknowledged to be the preferred target of ANCAs (Lüdemann, Utecht, & Gross, 1990).

How PR3 interacts with the plasma membrane of the neutrophils remains in facts a controversial subject. Several studies identified potential protein partners of PR3 at the membrane, among these potential partners are CD177 (NB1) (Hu et al., 2009; von Vietinghoff et al., 2007), Fcgamma receptor FcgRIIIb and $p22^{phox}$ subunit of cytochrome b558 (Alina David, Fridlich, & Aviram, 2005), β2 integrin adhesion molecule CD11b/CD18 (A David, Kacher, Specks, & Aviram, 2003), Protease Activated Receptor 2 (PAR2) (Jiang et al., n.d.; Kuckleburg & Newman, 2013) and Phospholipid Scramblase 1 (Kantari et al., 2007). The modalities of the membrane expression of PR3 are also depending on how neutrophils themselves are stimulated. A study made on cells has shown by quantitative fluorescence microscopy that PR3 is expressed at the surface of primed and activated neutrophils and that the level of PR3 membrane expression varies depending on which agonist is used to stimulate the neutrophils (Campbell et al., 2000). In addition to these experiments conducted on cellular models, a direct interaction between PR3 and liposomes had been reported by Goldmann et al. (Goldmann, Niles, & Arnaout, 1999). They studied the interactions between purified human PR3 with mixtures of zwitterionic and anionic reconstituted lipid bilayers using differential scanning calorimetry and lipid photolabeling and showed a direct interaction of PR3 with liposomes with dissociation constant (K_D) in the micromolar range. Understanding precisely the mechanisms with which PR3 binds to the surface of membrane and identifying, within the

cell membrane, which entities are responsible of the interaction and how there are involved, is thus of prior importance to modulate the expression of PR3 at the surface of cells.

Computational studies on PR3 and implicit membrane model, mimicking the surface of the lipidic surface, have predicted a membrane binding site of PR3 to the plasma membrane. This simplistic model shows that the interfacial binding site (IBS) is made of basic and hydrophobic amino acids act jointly to respectively orient and anchor PR3 at the surface of the plasma membrane (Hajjar, Mihajlovic, Witko-Sarsat, Lazaridis, & Reuter, 2008). The involvement of these amino acids have been confirmed by mutagenesis experiment, where mutations of the four hydrophobic (F180, F181, L228, F229) or four basic (R193, R194, K195, R227) amino acids abrogated the membrane anchorage of PR3 (Kantari et al., 2011). All-atom molecular dynamics simulations pointed out the detailed mechanisms of interaction between PR3 and lipid bilayers and showed the identified basic residues interacts via hydrogen bonds with the lipid headgroups to stabilize PR3, hydrophobic residues insert into the hydrophobic core below the carbonyl groups of the lipid bilayer and aromatic residues contribute to electrostatic interactions via cation π interaction with the choline group of phosphocholine (Broemstrup & Reuter, 2010). Computational studies are so far supporting the hypothesis of a direct binding.

The aim of this work is to show, both from a macromolecular level and an atomic level, that PR3 is able to directly bind lipid bilayers. We used Surface Plasmon Resonance Spectroscopy and molecular dynamic simulations for that purpose. We show that PR3 binds to 1-palmitoyl-2-oleosyl-sn-glycero-3-phosphocholine (POPC) liposomes, an artificial membrane model, and *in silico* POPC lipid bilayers, respectively through SPR experiments and MD simulations. POPC lipids are more relevant for physiological studies as being more fluid than other type of lipids such as DMPC. The simulation performed was conducted at a long timescale (500 ns) as it has be shown a longer timescale gives a better correlation with experiments (Grauffel et al., 2013).

Material & Methods

Proteins and phospholipids

PR3 and HNE were purchased from Athens Research & Technology and lipids (POPC) from Avanti Polar Lipids. Fatty acid free bovine serum albumine (BSA) was obtained from Sigma.

Liposome preparation

Liposomes were prepared as reported in (Jr, Ying, Baumann, & Kleppe, 2009). Lipids solvated in chloroform were added in glass tubes in prerequisite amount. Lipids were handled and kept out of light and reactive atmosphere by operation in hoods and using glass containers wrapped in aluminum foil. The chloroform solutions were dried under dry N_2 pressure. Traces of chloroform were removed by subjecting the samples to vacuum for at least two hours. Lipid cakes were rehydrated with HBS-N buffer and vortexed vigorously until no traces were left in the tubes. For liposomes preparation, solutions were subjected to seven freeze-thaw cycles using liquid N_2 and a warm water bath. The hydrated multilamellar structures were then extruded using a Mini-Extruder (Avanti Polar Lipids) assembled using two Millipore filters of 100 nm pore size. Samples were forced thought the filters 10 times using Hamilton syringes and the resulting solution were transferred to clean, foil wrapped glass tubes and stored at 4°C. Final liposome composition was 100 % POPC and were made at a concentration of 2.5 mM.

Affinity measurement using Surface Plasmon Resonance (SPR)

The SPR analyses were carried out on a BIAcore T200 (BIAcore, GE Healthcare) and Biacore T200 Control Software. All experiments were carried at 25° C. Protein and lipid interactions were monitored using a L1 sensor chip. Prime procedure was performed before each experiment. The surface of the L1 sensor ship was first cleaned with a 1 min injection of octylglucosyl 40 mM at a flow rate of 10 µl/min. Liposome solutions were diluted to 1 mM concentration with running buffer (HBS-N: 0.1 M HEPES, 1.5 M NaCl, pH 7.4) and injected at a flow rate of 1 µl/min for 10 minutes until maximum of binding was reached. Liposomes deposition resulted in 8500 RU for POPC. The surface of the L1 chip was then washed with a solution of NaOH 10 mM for 1min at a flow rate of 10 µl/min. The coverage of the chip was

accessed by injection of BSA 0.1 mg/ml at 10 µl/min for 60 s. Binding assays were performed. The two proteins (PR3 and HNE) were diluted to a set of at least 5 different concentrations ranging from 0 to 3 µM and were injected over the immobilized liposomes at a flow rate of 5 µl/min during 120 s to 180 s until the equilibrium was reached. Dissociation phase were measured for at least 480 s after the addition of the sample. At the end of the binding assay, the surface of the sensor chip was regenerated with a solution of octylglucosyl 40 mM for 30s at a flow rate of 30 µl/min. No reference channel was used due to high no specific binding and maximal coverage of the chip with liposome was achieved to fully cover the chip. The SPR data were analyzed with the Biacore T200 Evaluation Software. Binding affinities were calculated using the steady state affinity model (Langmuir model) and maximal resonance unit (RU) was plotted against concentration.

Intrinsic fluorescence spectroscopy (CHANGE TO FRET)

Measurements were performed as described in (Bustad, Underhaug, Halskau, & Martinez, 2011). Intensity of tryptophan fluorescence is measured using Perkin Elmer Luminescence Spectrometer LS50B and FL WinLab software with PR3 and HNE in HBS-N buffer, containing different amount of detergent [detergent type still have to be determined]. Measurements are performed at 25 C. at pH 7.4. Emission wavelength was chosen to be 295 nm in order to avoid the fluorescence from the tyrosine. Final protein concentration was 1 µM. An excitation wavelength of 295 nm was used, and excitation and emission slits were set to 5 nm. Emission spectra were collected 150 nm/min in the range of 310 to 420 nm and 2 sample parallels were acquired. Spectra of blank samples were subtracted to the main spectra.

Liposome binding assay

Protocol will be adapted from (Rosenbaum et al., 2011) if we decide to perform this experiment.

Molecular Dynamic Simulation of PR3 and POPC lipid bilayers

MD simulation of PR3 inserted in POPC lipid bilayers has been performed. The main steps of the procedure are the followings: (1) building of lipid bilayers with CHARMM-GUI and equilibration of the membrane (2) insertion of PR3 in the lipid bilayer according to the orientation described in (Hajjar et al., 2008) and (3) simulation of the complex PR3-POPC.

Simulation of POPC lipid bilayer

A lipid bilayer made of 256 POPC was build using CHARMM-GUI (Jo, Lim, Klauda, & Im, 2009). The lipid bilayer was then optimized with NAMD using the CHARMM36 force field (Klauda et al., 2010) and NAMD program. The system was then equilibrated for 300 ps at 310 K using a time step of 2 ps. The system was then run into production for 60 ns. The SHAKE algorithm was applied to constraint bonds between a heavy atom and a hydrogen (Andersen, 1983). Non-bonded interactions were truncated using a cutoff of 12 Å, using a switch function for van der Waals and a shift function for electrostatics and the Particle-Mesh-Ewald (PME) algorithm was used to estimate long-range electrostatic forces (Darden, York, & Pedersen, 1993; Essmann et al., 1995). The Langevin algorithm was used to control temperature (310K, damping coefficient: 10/ps) and pressure (target pressure: 1 atm, oscillation period: 75 fs, oscillation decay time: 25 fs) (Feller, Zhang, & Pastor, 1995). Two criteria have been used to access the biophysical properties of the POPC membrane. Surface area per lipid and order parameter were monitored along the simulation to ensure the stability of the membrane. The order parameter S_{CD} was calculated with VMD from the average value of the angle as:

$$S_{CD} = \left\langle \left(\frac{3}{2}\cos^2\theta - \frac{1}{2} \right) \right\rangle$$

The surface area was calculated to be 65.5 ± 0.8 Å on average during the simulation (cf. figure 4). A previous simulation of POPC lipid bilayer has shown a surface area of 64.7 ± 0.2 Å (Klauda et al., 2010) while the experimental estimate is 68.3 ± 1.5 Å (Kucerka, Tristram-Nagle, & Nagle, 2005). The order parameter of the two acyl chains of the lipid was calculated as described previously and is shown is figure 4. Profiles are consistent with those in (Klauda et al., 2010). (Check exp data >> only POPE????)

Simulation of PR3 inserted into POPC lipid bilayer

The Cartesian coordinates of PR3 were taken from chain A of the crystal structure referenced 1FUJ in the Protein Data Bank (Fujinaga, Chernaia, Halenbeck, Koths, & James, 1996). PR3 was then inserted into the equilibrated POPC lipid bilayer as described previously (Broemstrup & Reuter, 2010). Briefly, one copy of PR3 was inserted on the surface of the lipid bilayer according to the membrane binding orientation. PR3 was then translated 2 Å further apart from the lipid bilayer due to the width length between DMPC bilayers used

previously and the POPC bilayer used here. Overlapping lipids with the protein were removed. The system was then solvated into a cubic box of TIP3 water and neutralized with VMD (version 1.8.7) (Humphrey, Dalke, & Schulten, 1996) to avoid simulation in non-equilibrated system. The system was then minimized with CHARMM using first the steepest descent and then the conjugate gradient algoritms. Constraints were used on the backbone of the protein. The system was then equilibrated for 600 ps with NAMD. The Langevin algorithm was used to control temperature (310K, damping coefficient: 1/ps) and pressure (target pressure: 1 atm, oscillation period: 75 fs, oscillation decay time: 25 fs). Cutoff distances of 12 Å and a switching distance of 11 Å were applied on short range interactions (electrostatic and Van der Waals). Particle Mesh Ewald (PME) was used to estimate long range electrostatic interactions (Darden et al., 1993; Essmann et al., 1995). The integration of the equation of motion were done using a Multiple Time Step algorithm (Izaguirre, Reich, & Skeel, 1999); bonded interactions and short-range nonbonded forces were evaluated every step and long range electrostatics every second step The system was then run into production for 500 ns in the NPT ensemble.

Analyses

Root mean square deviation (RMSD) was calculated along the simulation as follow:

$$RMSD = \sqrt{\frac{\sum_{i=1}^{n} \|d_i\|^2}{n}}$$

Hydrogen bonds were calculated with Charmm using a 2.4 Å cutoff distance between hydrogen and acceptor and a 130° donor-hydrogen-acceptor angle criterion. The donor and acceptor are from the Charmm force field. Hydrophobic contacts were calculated using a 3 Å cutoff distance between the aliphatic group of the amino acid side chain (ca; cb; cg1; cg2; cg2; ha*; hb*; hg; hg2*; type cg except for hsd, hse, asn, asp; type hg1 except for cys, thr, ser; type cd except for arg, gln, glu; type cd1; type cd2 except for hsd, hse; type ce1, ce2, cz and associated hydrogens of phe, tyr, type cd1, cd2, ce2, ce3, cz2, cz3 and associated hydrogen of trp, type cay and type hy*). Cation-π interactions between aromatic rings (phenylalanine, tyrosine and tryptophan) are considered to exist when all distances between the atoms of the aromatic ring and choline nitrogen are below 7 Å and when these distances do not differ more than 1.5 Å (Chipot & Minoux, 1999; Petersen, Jensen, & Nielsen, 2005).

Results

Immobilization levels for of POPC liposomes on the L1 chip

Liposomes were immobilized on the surface of the L1 sensor chip at a low flow rate (1 $\mu L.min^{-1}$) until the maximal amount of deposition was reached. Liposome immobilization levels were monitored over time and immobilization level for POPC are 8563 ± 243 RU summarized in Table 1. To avoid non specific binding of proetins to the surface of the L1 chips, special care was taken on covering the chip surface at the highest possible levels of liposomes. The level of the coverage sensor chip was assessed with BSA injections (0.1 $mg.ml^{-1}$). Resulting signals from BSA around 100 RU or less indicates a sufficient coverage. In our case, BSA binds to around 12 RUs of the chip and allowed us to pursue experiments further with POPC.

Binding of PR3 to neutral liposomes

We investigated the interaction of PR3 with neutral liposomes made of POPC using SPR. Liposomes were flown over the surface of the L1 sensor chip as described above. Binding assays were performed by injecting protein samples at increasing concentration and affinity calculations were carried out by steady state analysis. Association phase was monitored during 180 s and dissociation phase was monitored 420 s. Sensorgrams show that the protein response is concentration dependant and is reaching the equilibrium at the end of each injection (Figure 1). The calculated K_D between PR3 and POPC is $9.24\ 10^{-7}$ M. During the dissociation phase, we also observed that the response signal of PR3 does not return to zero and thus demonstrate a persistent binding of PR3 to the liposomes. These results support the hypothesis of a direct binding of PR3 towards neutral liposomes (POPC).

Binding of HNE to neutral liposomes

The binding of HNE towards POPC was monitored in the same way as PR3. Association time was monitored for 120 s (not 180 s as for PR3) and dissociation time monitored for 420 s. Sensorgrams show that HNE can bind to liposome made of POPC in a concentration dependant manner which indicates a direct binding of the protein to the liposomes. During the dissociation phase, the signal drops immediately and returns to zero, as it is not observed for PR3, and shows a non-persistent binding. The kinetics of the protein-membrane interaction seems to be different for the two proteins. For the K_D calculation, the data collected for HNE clearly shows that the equilibrium was not reached under the used experimental conditions and due to limited availability for protein it was not possible to calculate the affinity accurately. Therefore, we hypothesized, from these experiments, a lower limit for the K_D of HNE towards POPC of approximately 3.41 μM.

Comparison between PR3 and HNE affinity towards neutral liposomes

PR3 and HNE affinity towards POPC were investigated using steady state analysis. Affinity constants are reported in Table 2.

Intrinsic fluorescence spectroscopy [Change to FRET]

Intrinsic fluorescence spectroscopy is used to (1) confirm measurements for PR3 and HNE and validate the affinity calculations and (2) obtain affinity data for fully negatively charged liposomes (POPS 100 %) as we do not obtain a good enough chip coverage to perform reliable SPR experiments. Indeed immobilization of fully negatively charged liposomes was showed to be difficult to achieve due to the nature of the L1 sensor chip (4882 RU immobilized for POPC:POPS 50:50 with BSA at 211 RUs). These experiments still require optimization since it seems that PR3 and HNE aggregate which yields a variable fluorescence signal.

Molecular Dynamic Simulation of PR3 and POPC lipid bilayers

MD simulations of POPC with/out PR3 were used to access the mode of interactions PR3 has with the lipid bilayers. We first prepared a lipid bilayer made of POPC and then performed the following analyses on the protein-membrane system: calculation of hydrogen bonds and hydrophobic contacts, cation π interactions.

Interaction between PR3 and POPC lipid bilayers

PR3 was embedded in the previously equilibrated POPC lipid bilayer and simulated by molecular dynamic simulations for a duration of 500 ns. Atomistic interactions between PR3 and the lipids were carefully examined. Hydrogen bond occupancy was calculated between PR3 and the POPC. Bonds with the phosphate group and the glycerol group were computed separately. Hydrogen bonds are formed with three different groups of residues (cf. Table 3 and Figure 6). Basic amino acids (K99, R177, K187, R186A, R186B and R222) show high contributions to the membrane binding via hydrogen bonding. These hydrogen bonds preferably occur with the phosphate group of the choline. To a lower extend, interaction occurs as well with the glycerol group, more deeply embedded in the membrane. Aromatic

residues (TRP218) and polar (THR161, THR164) residues interact via hydrogen bonding with the phosphate oxygen of the choline. TRP218 also interacts via the glycerol group of the lipid.

Hydrophobic contacts were also calculated and assessed with average interaction number per frame along the simulation and are represented in Figure 7 and Table 3. As show on the figure, an important number of residues from the interfacial binding site display hydrophobic contacts with the POPC lipid bilayer. The amino acid involved in hydrophobic contacts are of basic nature (LYS99, HIS132, HIS 147, ARG177, ARG186A, ARG222), hydrophobic nature (VAL163, PRO178, PRO186, ILE217, THR221, LEU223, PHE224, PH227) and aromatic nature (PHE165, PHE166, PHE184, TRP218, PHE215). Among the residues that have the highest lifetime percentage (above 75 %) are the three aromatic residues PHE 165, PHE166 and TRP218. These are the most embedded within the lipid bilayer. LEU223 seats as well on one of the most embedded loop in the protein, whereas the four hydrophobic residues VAL163, PRO186, ILE217 and LEU223 are located above these aromatic residues. High scoring ARG186A and ARG186B and LYS187 are located once again one level above the hydrophobic residues.

Both hydrogen bond and hydrophobic calculation show a strong interaction between PR3 and POPC lipid bilayers. These interactions, that occurs in the interfacial binding site, are maintained along the simulation. As membranes are flexible entities, their surfaces are not strictly ordered and fixed in space and the lipids can move within the bilayer, we captured the interactions between the lipid and the bilayers as an average number of interactions per frame (either for bonds and contacts).

Cation π interactions were calculated between aromatic residues located in the vicinity of the lipid bilayer and the choline nitrogen of the lipids upon the distance criteria described above. These calculations showed that two residues, TRP218 are the main actor in cation π formation (cf. Fig 6). Tryptophan residues are known to have a special role for membrane proteins since their tryptophan content is usually higher. TRP218 is known as being an important contributor to the membrane binding since it displays a significant participation towards hydrogen bonds and hydrophobic contacts. The lifetime of TRP218 cation π is 5.7 %.

Discussions & Conclusion

We report here experimental evidences of binding of PR3 to artificial membrane lipid bilayers and computational simulation that provide mechanistic details of the interaction mode. The direct binding of PR3 to phospholipid bilayers of zwitterionic nature was confirmed by SPR. This data confirm that PR3 can bind POPC liposomes at an affinity (K_d) of 0.92 10^{-6} M. Your results also demonstrate that HNE can bind to zwitterionic bilayers, but to a lower strength. High amounts of HNE would have been necessary to capture the binding affinity with high precision. We thus estimated a lower limit of 3.41 10^{-6} M. Comparison of PR3 and HNE binding properties showed that both of these proteins could bind zwitterionic bilayers, PR3 showing a stronger association. Moreover, visual estimates of association and dissociation rates of PR3 seem to be slower than for HNE and indicate a stronger and more permanent interaction for PR3 than HNE towards zwitterionic liposomes. Kinetics calculations have not been performed in our case due to the slow injection rate used for both of the proteins (5 $\mu l.min^{-1}$) that could create high mass transport effect and thus inaccurate kinetic data. Moreover, HNE completely dissociates from the liposomes, whereas PR3 stays at the surface of the liposomes, thus suggesting differences in binding mechanisms of these two proteins. It has been experimentally showed that PR3 is more likely to be eluted from cell membrane than HNE by solutions of low ionic strength because PR3 is a less cationic enzyme in comparison that HNE (Campbell et al., 2000). This fact seems to reflect on the sensorgrams shape from these two enzymes.

It has been suggested that PR3 can directly bind to neutral membrane model and that the strength of binding was stronger for PR3 compared with HNE, the latest was described as a non binding protein, results that are in qualitative agreement with our work (Goldmann et al., 1999). However, the Kd previously reported by Goldman showed that PR3 could bind DMPC liposomes at 85 10^{-6} M, that is about a hundred time more than what we measured (Goldmann et al., 1999). The data we obtained by SPR show that PR3 can directly bind zwitterionic lipids. Substantial amounts of HNE binds to neutral liposomes as well but the affinity towards this kind of liposomes is lower that for PR3. The fact that HNE can dissociate from the POPC can be explained based on previous structural study (Hajjar et al., 2008). This study indicated that PR3 and HNE, two homolog proteins, share a similar fold, although the charge distribution at their surfaces is quite different (Hajjar, Broemstrup, Kantari, Witko-

Sarsat, & Reuter, 2010). It has been described that HNE interaction with the membrane is driven mainly by basic residues and possess less hydrophobic residues in the IBS than PR3. Since hydrophobic residues insert more deeply in the membrane, a lack of these residues in HNE case could suggest a more superficial mode of interactions.

SPR protocol was carefully designed for PR3/HNE affinity measurement towards POPC. The full coverage of the sensor chip with liposomes was achieved with low injection rate and long injection time and to ensure optimal coverage of the chip, BSA was flown over the covered chip and had almost no binding, thus eliminating non specific binding of protein to the L1 chip. No reference channel was used due to non negligible non specific binding of your proteins toward the chip, as mentioned previously. Affinity was calculated only when the equilibrium was reached.

Molecular dynamic simulations of PR3 anchored at the surface of a POPC lipid bilayer showed that PR3 interacts directly with the lipids via hydrogen bonds, hydrophobic contact and cation π interactions. Our simulations identified basic (K99, R177, K187, R186A, R186B and R222) and aromatic residues (PHE165, PHE166, TRP218) and polar (THR161, THR164) as contributing residues involved in hydrogen bonds. Hydrophobic contacts between PR3 and POPC involve residues of basic (LYS99, HIS132, HIS 147, ARG177, ARG186A, ARG222), hydrophobic (VAL163, PRO178, PRO186, ILE217, THR221, LEU223, PHE224, PH227) and aromatic nature (PHE165, PHE166, PHE184, TRP218, PHE215). All-atom molecular dynamic simulations also showed direct interaction between PR3 and three different types of lipid bilayer made of DMPC, DMPG or a mixture of DMPC and DMPG (Broemstrup & Reuter, 2010). These simulations showed that five basic residues (R177, R186A, R186B, K187, R222) and six hydrophobic residues (F165, F166, F224, L223, F184, W218) were implicated in the membrane binding. Hydrogen bond patterns described between PR3 and POPC are in agreement with previous simulations made with DMPC, DMPG or an equimolar mixture of DMPC/DMPG membrane.

Amphitropic proteins such as PR3 bind transiently to membrane, usually via a charged mechanism. It has been established that the binding of proteins such as Scr or K-Ras is mediated via non specific electrostatic interactions. Electrostatic potential from protein surfaces can provide the driving force to orient the protein at the surface of the membrane (Cho & Stahelin, 2005; Mulgrew-Nesbitt et al., 2006). The role of the charged residues,

especially of basic nature, is thus of crucial importance in the binding process of these proteins, and was demonstrated here. Indeed, a set of basic residues in PR3 (K99, R177, K187, R186A, R222, and R230) are often involved in hydrogen bonding with the phosphate group of the lipids, and also with hydrophobic contacts. Basic residues are thus providing a strong interaction network in PR3 anchorage. The role of these amino acids has also been demonstrated through implicit membrane simulation where a set of basic residues was described as key residues of interaction. R177 and R186A especially were showing high contribution to membrane binding in terms of energy (Hajjar et al., 2008). These interactions, in the case of PR3, occur at the surface of the lipid bilayer. Aromatic residues, such as phenylalanine and tryptophan, penetrate more deeply into the membrane core and contribute to further stabilization of the protein anchorage. Hydrophobic residues insert into the membrane at an intermediate level between basic and aromatic amino acids (reformulate?) and display a significant number of hydrophobic contacts. The influence of these amino acids is of high importance and has been shown here with VAL163, ILE217 and LEU223. The latest is one of the highest contributors to the membrane binding as shown (Hajjar et al., 2008).

All together, these results are consistent with the hypothesis that PR3 can directly bind to artificially reconstituted lipid bilayer made of POPC.

Figures & Tables

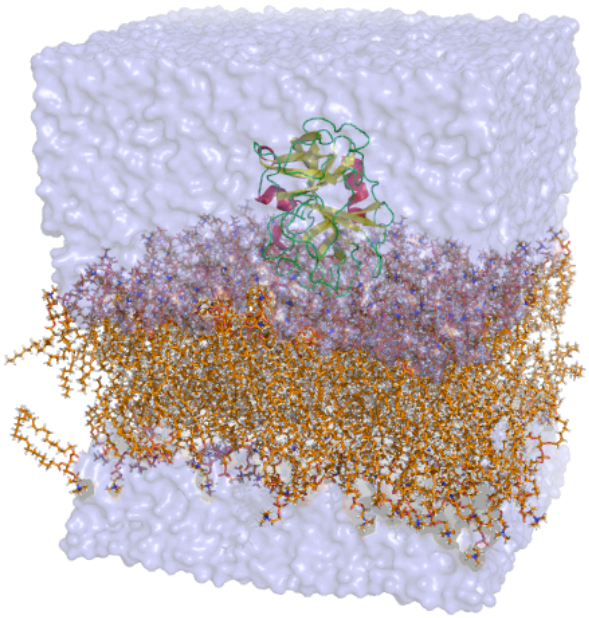

Figure 1: System setup for MD simulation. PR3 (carton representation colored by secondary structure element) was inserted into the POPC lipid bilayer (sticks representation colored by atom type). Protein and membrane are solvated into a water box (surface representation colored in blue)

Table 1: Affinity calculation of PR3 and HNE on different kind of liposomes.

Liposome type	Affinity ($x10^{-7}$ M)	
	PR3	HNE
POPC	9.24 ± 0.60	34.1

Table 2: Liposomes immobilization levels (POPC, POPC:POPS 50:50) and chip coverage accession by BSA binding (BSA is used at 0.1 mg/ml and is injected 60 s at 60 $l.min^{-1}$).

Liposome type	Immobilization level (RU)	BSA binding level (RU)
POPC	8563 ± 243	12.6
POPC:POPS 50:50	4882	211

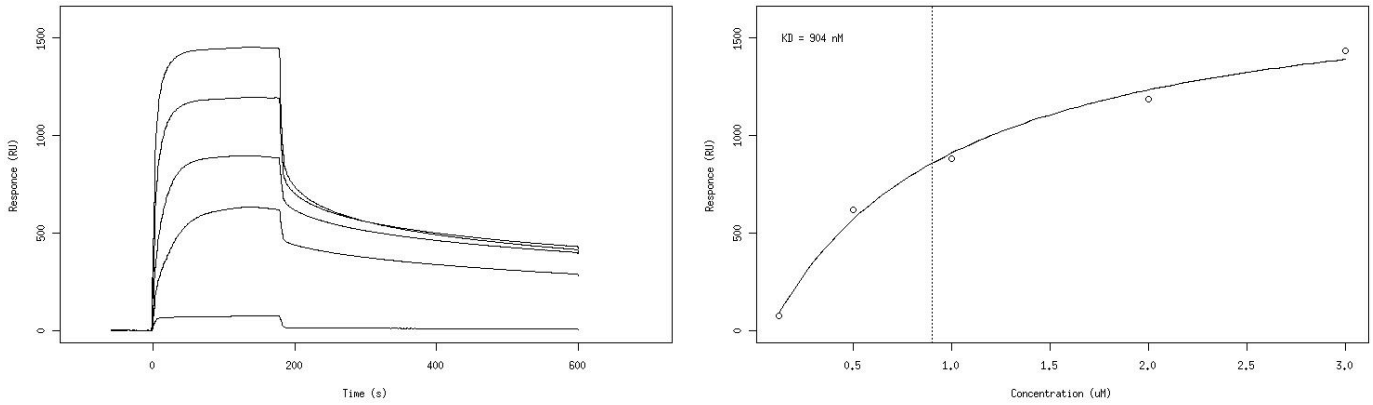

Figure 2: PR3 binding responses (left) and affinity data (right) over immobilized POPC. All data are blank substracted. No double referencing has been done due to high non specific binding to the reference channel (L1 chip with no liposomes – data not shown).

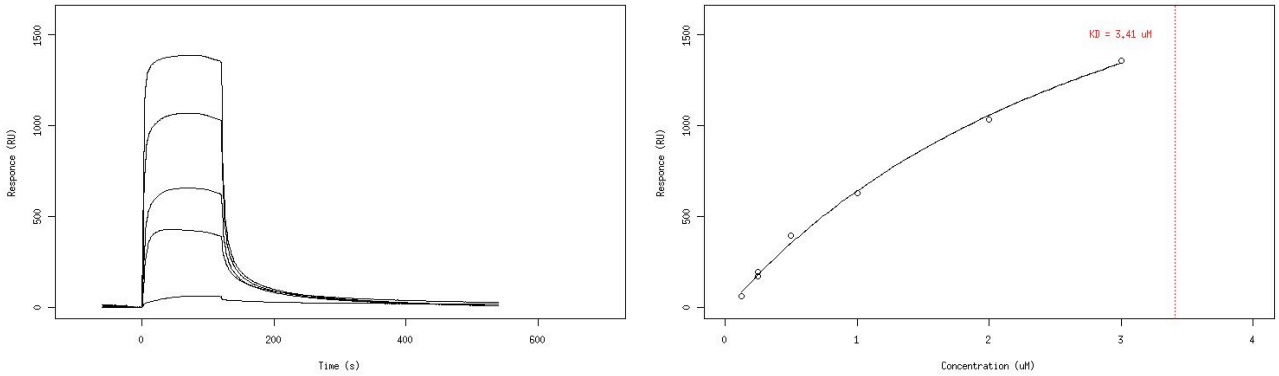

Figure 3: HNE binding responses (left) and steady state (right) over immobilized POPC. All data are blank substracted. No double referencing has been done due to high non specific binding to the reference channel (L1 chip with no liposomes – data not shown).

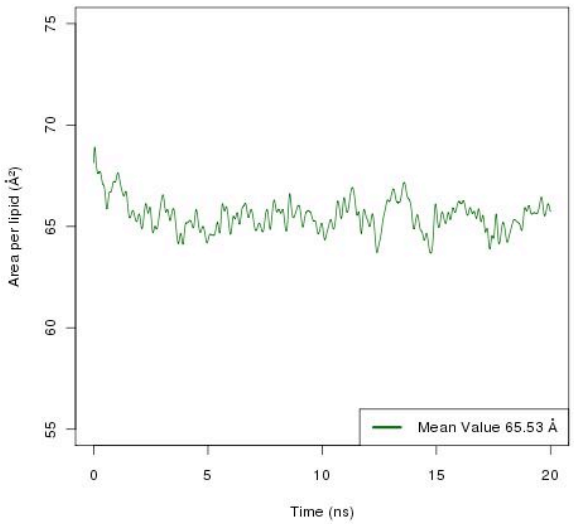

Figure 4: Area per lipid calculated through time

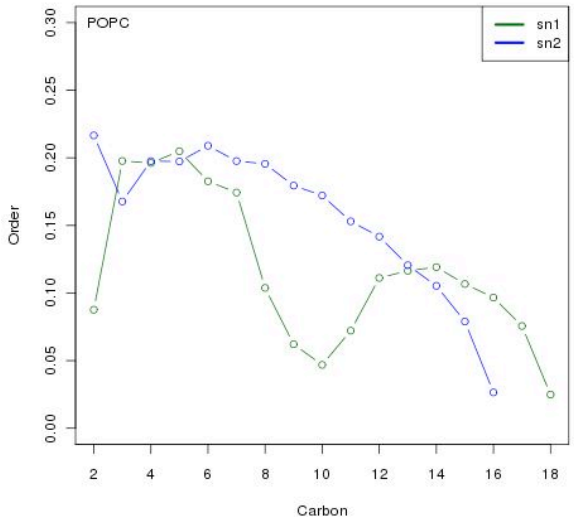

Figure 5: Order parameter

Table 3 Summary of interactions between PR3 and POPC lipid bilayer. Hydrogen bonds with lipid phosphate groups (black) or glycerol group (G), hydrophobic contacts (if <1)

Residue	Hydrogen bond (% occupancy)	Hydrophobic contact (average # contact per frame)	Depth of anchorage (Å)	Cation π (% occupancy)
LYS99	20.1 P		- 11.2 ± 2.1	
HSD132	12.6 P / 6.8 G		- 2.9 ± 2.7	
THR161	16.5 P		- 4.7 ± 1.8	
VAL163		2.3	- 2.5 ± 1.6	
THR164	45.6 P		- 1.7 ± 1.6	
PHE165		1.5	+ 1.8 ± 1.5	
PHE166	28.1 P	2.5	+ 1.7 ± 1.6	
ARG177	87.9 P	1.1	- 4.0 ± 1.6	
ARG186A	85.9 P / 20.6 G	4.2	+ 0.7 ± 2.1	
ARG186B	82.9 P	1.5	- 1.3 ± 2.2	
LYS187	74.5 P / 90.4 P	1.6	- 0.2 ± 2.4	
PHE215			- 8.6 ± 2.0	5.9
TRP218	12.8 P / 26.6 P	1.9	+ 0.8 ± 2.3	5.7
ARG222	8.8 P		+ 0.9 ± 2.0	
THR221		1.6	+ 0.1 ± 2.1	
LEU223		5.8	+ 3.5 ± 1.9	
PHE224		1.2	+ 1.2 ± 1.8	
PRO225		1.9	- 1.6 ± 1.7	

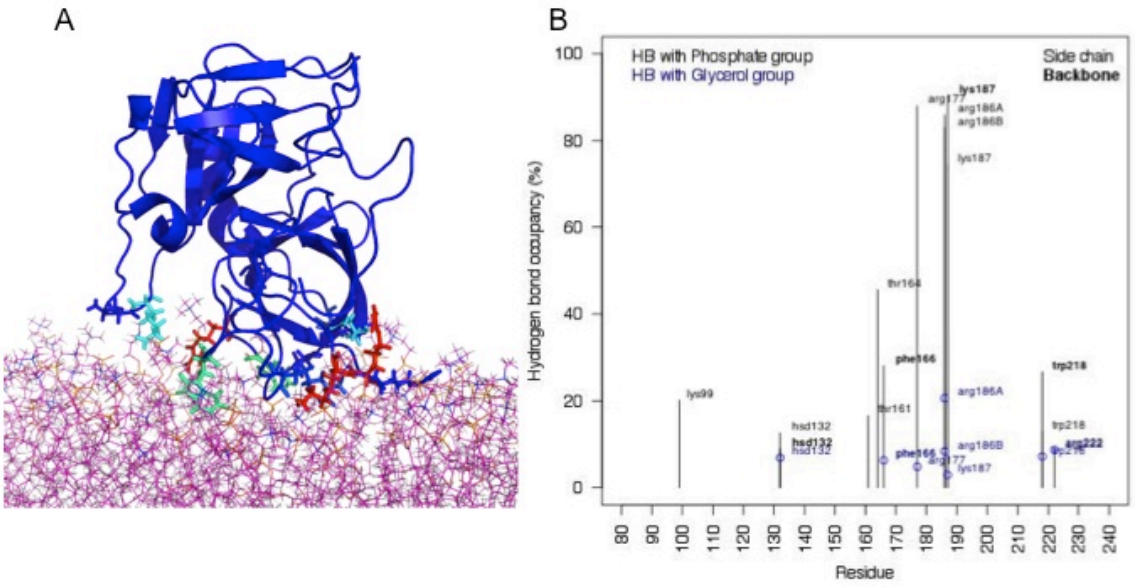

Figure 6: Hydrogen bond calculation between PR3 and POPC. Left figure shows the main HB contributors in sticks representation (colored by percentage of occupancy) – membrane is shown in lines and protein in cartoon. Right figure shows the occupancy of hydrogen bond display by residue.

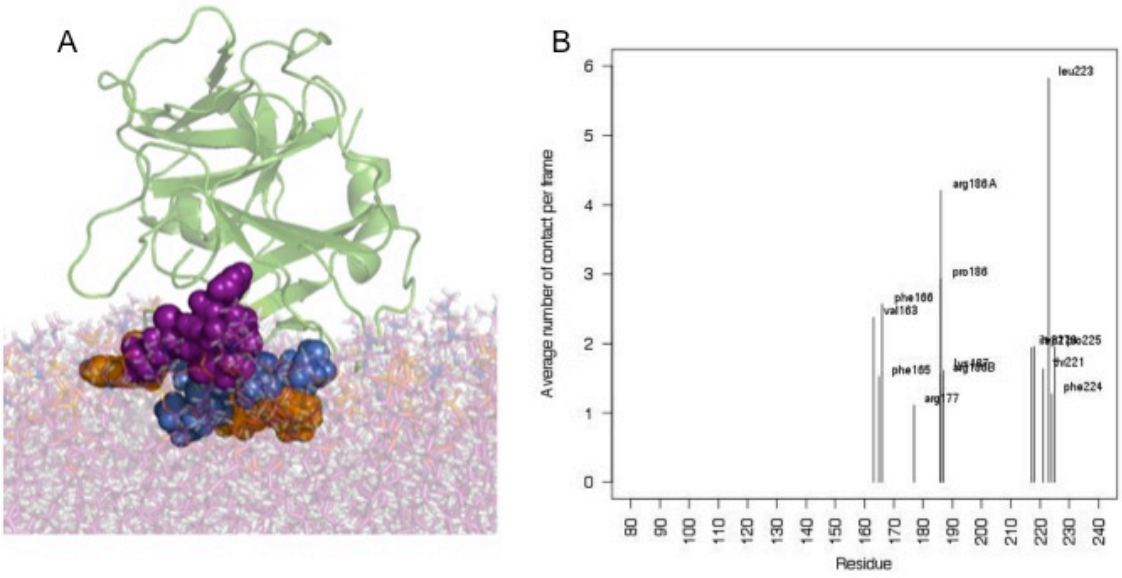

Figure 7: Hydrophobic contact calculation between PR3 and POPC. Left figure represent all residues involved in hydrophobic contacts (purple, blue and orange spheres for respectively basic, hydrophobic and aromatic residues). PR3 is represented is carton and POPC lipid bilayer in sticks. Right figure shows the lifetime of hydrophobic contact display by residue.

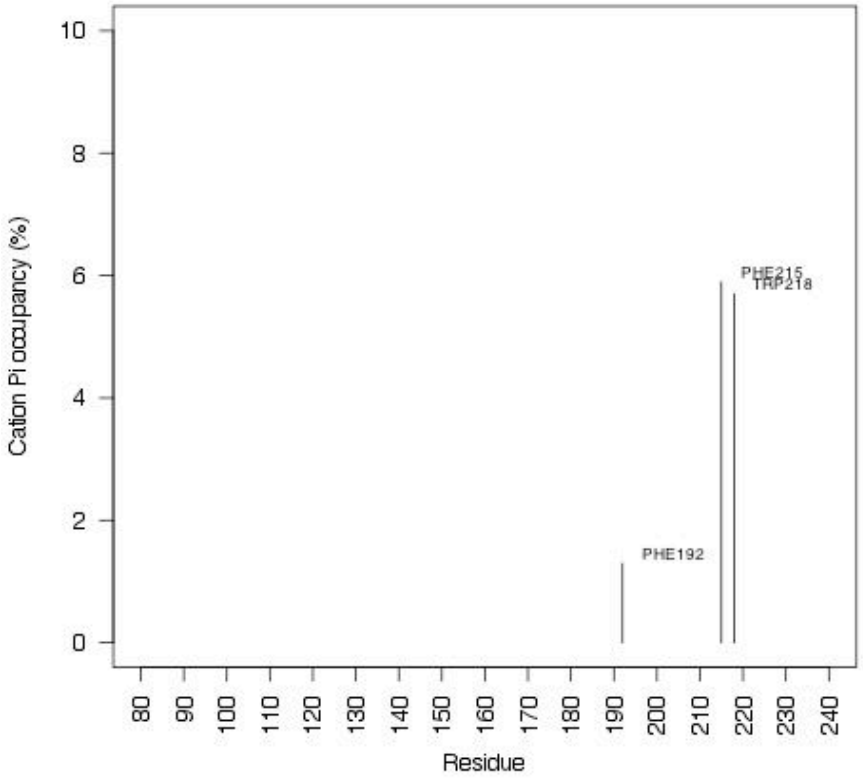

Figure 8: Cation π interactions between PR3 and the lipid bilayers.

References

Andersen, C. (1983). Rattle : A " Velocity " Molecular Version of the Shake Dynamics Calculations for. *Journal of Computational Physics*, 24-34.

Baggiolini, M., Bretz, U., Dewald, B., & Feigenson, M. E. (1978). The polymorphonuclear leukocyte. *Agents and actions*, *8*(1-2), 3-10. Retrieved from http://www.ncbi.nlm.nih.gov/pubmed/345782

Broemstrup, T., & Reuter, N. (2010). How does proteinase 3 interact with lipid bilayers? *Physical chemistry chemical physics : PCCP*, *12*(27), 7487-96. doi:10.1039/b924117e

Bustad, H. J., Underhaug, J., Halskau, O., & Martinez, A. (2011). The binding of 14-3-3γ to membranes studied by intrinsic fluorescence spectroscopy. *FEBS letters*, *585*(8), 1163-8. doi:10.1016/j.febslet.2011.03.027

Campbell, E. J., Campbell, M. A., & Owen, C. A. (2000). Bioactive Proteinase 3 on the Cell Surface of Human Neutrophils: Quantification, Catalytic Activity, and Susceptibility to Inhibition. *J. Immunol.*, *165*(6), 3366-3374. Retrieved from http://www.jimmunol.org/cgi/content/abstract/165/6/3366

Chipot, C., & Minoux, H. (1999). Cation-π Interactions in Proteins : Can Simple Models Provide an Accurate Description ? *Journal of American Chemical Society*, *121*, 10366-10372.

Cho, W., & Stahelin, R. V. (2005). Membrane-protein interactions in cell signaling and membrane trafficking. *Annual review of biophysics and biomolecular structure*, *34*, 119-51. doi:10.1146/annurev.biophys.33.110502.133337

Darden, T., York, D., & Pedersen, L. (1993). Particle mesh Ewald: An N · log(N) method for Ewald sums in large systems. *Journal of Chemical Physics*, *98*(12), 10089-10092. AIP. doi:10.1063/1.464397

David, A, Kacher, Y., Specks, U., & Aviram, I. (2003). Interaction of proteinase 3 with CD11b/CD18 (β2 integrin) on the cell membrane of human neutrophils. *Journal of leukocyte …*, *74*(October), 551-557. doi:10.1189/jlb.1202624.Journal

David, Alina, Fridlich, R., & Aviram, I. (2005). The presence of membrane Proteinase 3 in neutrophil lipid rafts and its colocalization with FcgammaRIIIb and cytochrome b558. *Experimental cell research*, *308*(1), 156-65. doi:10.1016/j.yexcr.2005.03.034

Essmann, U., Perera, L., Berkowitz, M. L., Darden, T., Lee, H., & Pedersen, L. G. (1995). A smooth particle mesh Ewald method, *103*(November), 31-34.

Feller, S., Zhang, Y., & Pastor, R. (1995). Constant-pressure molecular-dynamics simulation-the Langevin piston method. *Journal of Chemical Physics*, *103*(11), 4613-4621. Retrieved from http://www.cheric.org/research/tech/periodicals/view.php?seq=116765

Fujinaga, M., Chernaia, M. M., Halenbeck, R., Koths, K., & James, M. N. (1996). The crystal structure of PR3, a neutrophil serine proteinase antigen of Wegener's granulomatosis antibodies. *Journal of molecular biology*, *261*(2), 267-78. doi:10.1006/jmbi.1996.0458

Goldmann, W. H., Niles, J. L., & Arnaout, M. A. (1999). Interaction of purified human proteinase 3 (PR3) with reconstituted lipid bilayers. *European Journal of Biochemistry*, *261*(1), 155–162. Berlin; New York: Published by Springer-Verlag on behalf of the Federation of European Biochemical Societies, 1967-2004. Retrieved from http://www.biomed.uni-erlangen.de/lpmt/pubs_Wolfgang/EJB_261_99.pdf

Grauffel, C., Yang, B., He, T., Roberts, M. F., Gershenson, A., & Reuter, N. (2013). Cation – π Interactions As Lipid-Specific Anchors for Phosphatidylinositol-Specific Phospholipase C. *Journal of the American Chemical Society*, *135*, 5740-5750. Retrieved from http://pubs.acs.org/doi/full/10.1021/ja312656v

Hajjar, E., Broemstrup, T., Kantari, C., Witko-Sarsat, V., & Reuter, N. (2010). Structures of human proteinase 3 and neutrophil elastase--so similar yet so different. *The FEBS journal*, *277*(10), 2238-54. doi:10.1111/j.1742-4658.2010.07659.x

Hajjar, E., Mihajlovic, M., Witko-Sarsat, V., Lazaridis, T., & Reuter, N. (2008). Computational prediction of the binding site of proteinase 3 to the plasma membrane. *Proteins*, *71*(4), 1655-69. doi:10.1002/prot.21853

Hu, N., Westra, J., Huitema, M. G., Bijl, M., Brouwer, E., Stegeman, C. a, Heeringa, P., et al. (2009). Coexpression of CD177 and membrane proteinase 3 on neutrophils in antineutrophil cytoplasmic autoantibody-associated systemic vasculitis: anti-proteinase 3-mediated neutrophil activation is independent of the role of CD177-expressing neutrophils. *Arthritis and rheumatism*, *60*(5), 1548-57. doi:10.1002/art.24442

Humphrey, W., Dalke, A., & Schulten, K. (1996). VMD: visual molecular dynamics. *Journal of molecular graphics*, *14*(1), 33–38. Elsevier. Retrieved from http://linkinghub.elsevier.com/retrieve/pii/0263785596000185

Izaguirre, J. a., Reich, S., & Skeel, R. D. (1999). Longer time steps for molecular dynamics. *The Journal of Chemical Physics*, *110*(20), 9853-9864. doi:10.1063/1.478995

Jiang, B., Grage-Griebenow, E., Csernok, E., Butherus, K., Ehlers, S., Gross, W. L., & Holle, J. U. (n.d.). The role of proteinase 3 (PR3) and the protease-activated receptor-2 (PAR-2) pathway in dendritic cell (DC)

maturation of human-DC-like monocytes and murine DC. *Clinical and experimental rheumatology*, *28*(1 Suppl 57), 56-61. Retrieved from http://www.ncbi.nlm.nih.gov/pubmed/20412704

Jo, S., Lim, J. B., Klauda, J. B., & Im, W. (2009). CHARMM-GUI Membrane Builder for mixed bilayers and its application to yeast membranes. *Biophysical journal*, *97*(1), 50-8. doi:10.1016/j.bpj.2009.04.013

Jr, Ying, M., Baumann, A., & Kleppe, R. (2009). Three-way interaction between 14-3-3 proteins, the N-terminal region of tyrosine hydroxylase, and negatively charged membranes. *Journal of Biological*, *284*(47), 32758 -32769. doi:10.1074/jbc.M109.027706

Kantari, C., Millet, A., Gabillet, J., Hajjar, E., Broemstrup, T., Pluta, P., Reuter, N., et al. (2011). Molecular analysis of the membrane insertion domain of proteinase 3, the Wegener's autoantigen, in RBL cells: implication for its pathogenic activity. *Journal of leukocyte biology*, *90*(5), 941-50. doi:10.1189/jlb.1210695

Kantari, C., Pederzoli-Ribeil, M., Amir-Moazami, O., Gausson-Dorey, V., Moura, I. C., Lecomte, M.-C., Benhamou, M., et al. (2007). Proteinase 3, the Wegener autoantigen, is externalized during neutrophil apoptosis: evidence for a functional association with phospholipid scramblase 1 and interference with macrophage phagocytosis. *Blood*, *110*(12), 4086-95. doi:10.1182/blood-2007-03-080457

Klauda, J. B., Venable, R. M., Freites, J. A., O'Connor, J. W., Tobias, D. J., Mondragon-Ramirez, C., Vorobyov, I., et al. (2010). Update of the CHARMM all-atom additive force field for lipids: validation on six lipid types. *The journal of physical chemistry. B*, *114*(23), 7830-43. doi:10.1021/jp101759q

Kucerka, N., Tristram-Nagle, S., & Nagle, J. F. (2005). Structure of fully hydrated fluid phase lipid bilayers with monounsaturated chains. *The Journal of membrane biology*, *208*(3), 193-202. doi:10.1007/s00232-005-7006-8

Kuckleburg, C. J., & Newman, P. J. (2013). Neutrophil proteinase 3 acts on protease-activated receptor-2 to enhance vascular endothelial cell barrier function. *Arteriosclerosis, thrombosis, and vascular biology*, *33*(2), 275-84. doi:10.1161/ATVBAHA.112.300474

Lüdemann, J., Utecht, B., & Gross, W. L. (1990). Anti neutrophil cytoplasm antibodies in wegener's granulomatosis recognize an elastinolytic enzyme. *The Journal of experimental medicine*, *171*(1), 357-362. Rockefeller Univ Press. Retrieved from http://jem.rupress.org/content/171/1/357.abstract

Mulgrew-Nesbitt, A., Diraviyam, K., Wang, J., Singh, S., Murray, P., Li, Z., Rogers, L., et al. (2006). The role of electrostatics in protein-membrane interactions. *Biochimica et biophysica acta*, *1761*(8), 812-26. doi:10.1016/j.bbalip.2006.07.002

Petersen, F. N. R., Jensen, M. Ø., & Nielsen, C. H. (2005). Interfacial tryptophan residues: a role for the cation-pi effect? *Biophysical journal*, *89*(6), 3985-96. doi:10.1529/biophysj.105.061804

Rosenbaum, S., Kreft, S., Etich, J., Frie, C., Stermann, J., Grskovic, I., Frey, B., et al. (2011). Identification of novel binding partners (annexins) for the cell death signal phosphatidylserine and definition of their recognition motif. *The Journal of biological chemistry*, *286*(7), 5708-16. doi:10.1074/jbc.M110.193086

Witko-sarsat, V., Lesavre, P., Lopez, S., Bessou, G., Hieblot, C., Prum, B., Unfeld, J.-pierre G. R., et al. (1999). A Large Subset of Neutrophils Expressing Membrane Proteinase 3 Is a Risk Factor for Vasculitis and Rheumatoid Arthritis. *World Health*, 1224 -1233.

Woude, F. V. der, Lobatto, S., Permin, H., Van Der Giessen, M., Rasmussen, N., Wiik, A., Van ES, L., et al. (1985). Autoantibodies against neutrophils and monocytes: tool for diagnosis and marker of disease activity in Wegener's granulomatosis. *The Lancet*, *325*, 425-429. Retrieved from http://www.sciencedirect.com/science/article/pii/S014067368591147X

von Vietinghoff, S., Tunnemann, G., Eulenberg, C., Wellner, M., Cristina Cardoso, M., Luft, F. C., & Kettritz, R. (2007). NB1 mediates surface expression of the ANCA antigen proteinase 3 on human neutrophils. *Blood*, *109*(10), 4487-93. doi:10.1182/blood-2006-10-055327